

Distribution of Loss Volume and Estimation of Loss for Aggregated Video Traffic

Astrid Undheim and Peder J. Emstad

Centre for Quantifiable Quality of Service in Communication Systems*

Norwegian University of Science and Technology, Trondheim, Norway

e-mail: {astrid, peder}@q2s.ntnu.no

Abstract—Estimation of the packet loss for a video transmission over a communication network is an important step for assessing the QoS perceived by the users. The loss probability is particularly important, but also the characteristics of the loss periods have a significant effect, since bursty losses influence the perceived QoS in a different way than uniformly distributed losses. In this paper, the video traffic is modeled as a discrete multivariate Gaussian process, taking the correlation between consecutive frames into account. Exceedances of frame sizes over a threshold constitute loss periods, and the distribution of the length of a loss period is found in an earlier work. Here, the distribution of the loss volume in a loss period is pursued using a numerical approach, giving the packet loss in the bufferless case. It is then shown how the loss volume can be employed to estimate the packet loss in a bottleneck node with small buffers.

Furthermore, relations between loss period characteristics for discrete and continuous Gaussian processes are investigated. In particular, it is found that a relation between the length and volume of excursions over high thresholds for a continuous process is valid for a discrete process as well.

Index Terms—Video traffic model, loss period, Multivariate normal integral

I. INTRODUCTION

With the increasing popularity of web-based video streaming services such as YouTube, the amount of video traffic transmitted over the Internet is enormous. For evaluating the Perceived Quality of Service (PQoS) for a video transmission, both the video content, different choices made in the encoder as well as network and multimedia impairments will have an influence, as discussed in [1]. In a recent paper [2], packet based metrics are seen as a viable solution for the objective evaluation of the PQoS. For video traffic, bursty losses influence the PQoS in a different way than uniform distributed losses, as is investigated e.g., in [3], [4]. The burstiness of losses can be assessed using loss periods, where a loss period consists of exceedances of frame sizes over a threshold as shown in Fig. 1(a). The length and loss volume of a loss period are then of great importance and can be used to deduce the PQoS for a video transmission over a network.

To accurately grasp the distribution of the length and loss volume of a loss period, it is necessary to apply a model that takes the covariance function of the traffic stream into account. Also, it is of paramount interest to choose a parsimonious model

and a model that can model an aggregate based on similar models of its single streams. The Gaussian process is attractive for modeling purposes thanks to its additive properties. Gaussian processes with independent increments have since long been used to model queueing type systems. Fractional Brownian Motion models, with dependent increments, have become popular to model long-range dependencies [5], however the covariance function must match that of Fractional Gaussian Noise (FGN) to apply this model. In [6], video traffic encoded using the enhanced H.264/AVC slice-based video encoding scheme [7] is modeled using a discrete multivariate Gaussian process. The first and second moments of the length of a loss period, i.e., periods where the frame sizes exceed a given threshold, are found. Relations between these moments for single and aggregated video streams are derived. In this paper, the loss volume of a loss period is studied. For a bufferless node, the total loss will be equal to the loss volume. In addition, an approach to packet loss estimation for a bottleneck node with a small buffer is developed, using the distribution of the loss volume in the bufferless case.

Characterization of the loss period can be seen as a level-crossing problem, for which there are very few general results. Level-crossing problems have been studied for Gaussian processes in [8] and experimental problems are investigated in [9]. In [10], different aspects of the level-crossing problems for first-order Markov processes are studied and relationships between discrete and continuous processes are given. Previous work on continuous Gaussian processes in [11] gives the limit distribution functions of the length, volume, and maximum height of excursions over high thresholds.

In this paper, an approximate formula is derived for the distribution of the loss volume of a loss period for the discrete Gaussian process, based on a numerical study. The Multivariate Normal Integral (MVNI) is solved numerically using the method developed in [12]. Furthermore, the application of the results for the continuous Gaussian process in [11] to video traffic is studied. The term excursion is used for exceedances over a threshold for the continuous process, while the term loss period is used for the exceedances in the discrete case as shown in Fig. 1. There is a difference between the discrete and the continuous process since a loss period of the former has a minimum length of 1, while there is no minimum for the continuous process.

The results from the numerical computation of the loss

*“Centre for Quantifiable Quality of Service in Communication Systems, Centre of Excellence” appointed by The Research Council of Norway, funded by the Research Council, NTNU and UNINETT. <http://www.q2s.ntnu.no>

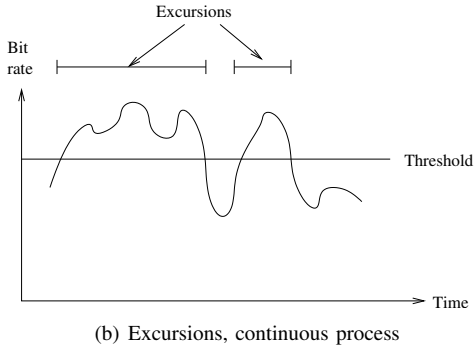
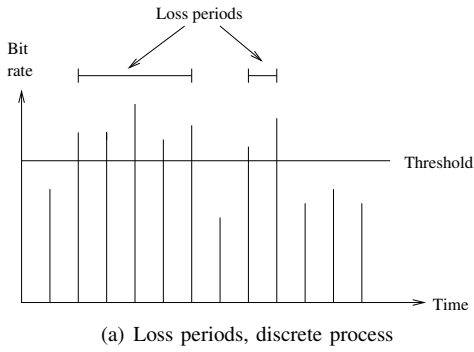


Fig. 1. Characteristics of exceedances.

volume for the discrete process are compared to the results for the continuous process as well as results from simulation of a flow. Based on the results in [11], a relation between the distributions of the length and volume of an excursion can be derived for the continuous process. This relation is checked for the discrete process as well.

The rest of this paper is organized as follows. The excursion characteristics for the continuous process are described in Section II and the requirements for the correlation function for the continuous process are investigated. The approach for estimating the loss volume of a loss period numerically is given in Section III, in addition to results from simulations. Section IV compares the first moments of an excursion and a loss period for a suitable correlation function. Little's formula is used as an alternative method for estimating the first moment of the length of an excursion and a loss period in Section V. The calculation of the loss in a model with finite buffer, using the distribution of the loss volume of a loss period in the bufferless case, is then given in Section VI. Finally, the paper is concluded in Section VII.

II. CHARACTERISTICS OF EXCURSIONS

A. Limit Distributions for Characteristics of Excursions

Expressions for the limit distributions of characteristics of excursions over a high level, such as length, volume and height of an excursion, are found for a Gaussian process in [11]. The process has zero mean and the exceedances are evaluated with respect to the level r when $r \rightarrow \infty$, where Δ_r is the length of an excursion, m_r is the maximum height of an excursion and S_r is the area of an excursion as shown in Fig. 2.

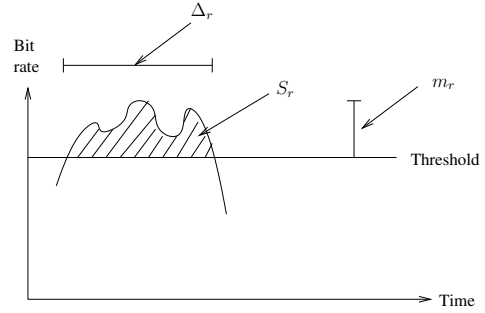


Fig. 2. The characteristics of excursions for a continuous process.

The distribution functions for the excursion statistics over a high threshold r are then given as:

$$P_1(v) = P\{r\Delta_r \geq v\} = \exp\left\{-\frac{\lambda_2}{8\lambda_0^2}v^2\right\}$$

$$P_2(v) = P\{rm_r \geq v\} = \exp\left\{-\frac{v}{\lambda_0}\right\}$$

$$P_3(v) = P\left\{\frac{3}{2}r^2S_r \geq v\right\} = \exp\left\{-\left(\frac{\lambda_2}{8\lambda_0^4}\right)^{1/3}v^{2/3}\right\}$$

where λ_k is given by:

$$\lambda_k = \int_0^\infty \lambda^k f(\lambda) d\lambda \quad (1)$$

where $f(\lambda)$ is the spectral density function of the autocorrelation of the process.

The spectral density for an autocorrelation function $\rho(t)$ is given as:

$$f(\lambda) = \frac{2}{\pi} \int_0^\infty \cos(\lambda t) \rho(t) dt. \quad (2)$$

The complementary cumulative distribution function (CDF) of Δ_r is used for calculating the moments of the length of an excursion. For the continuous distributions, the i -th order moments are defined using the complementary CDF as [13]:

$$E[r\Delta_r^i] = \int_0^\infty i \cdot v^{i-1} P_1(v) dv$$

and similarly for the volume and maximum height of an excursion.

In addition, the relationship between the distribution functions of the length and volume of an excursion is explored. It can be seen from (1) and (2) that λ_0 is always equal to 1, hence:

$$P_1(v) = \exp\left\{-\frac{\lambda_2}{8}v^2\right\}$$

and

$$P_3(v) = \exp\left\{-\left(\frac{\lambda_2}{8}\right)^{1/3}v^{2/3}\right\}.$$

Taking the natural logarithm of both of them gives:

$$P_3(v) = \exp\left\{-\left(-\ln P_1(v)\right)^{1/3}\right\} \quad (3)$$

and hence a very simple relation between the distribution functions of the two characteristics exists. This relation is

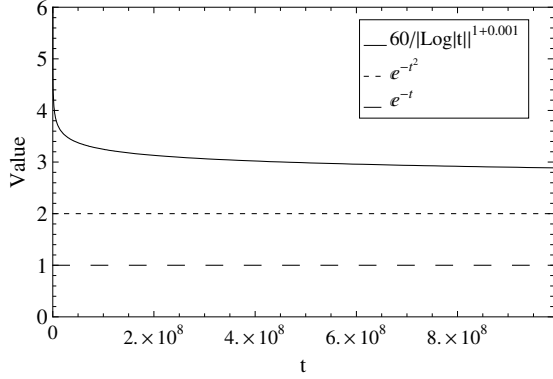


Fig. 3. $|\rho''(0) - \rho''(t)|$ versus $\psi(t) = C/|\log |t||^{1+\epsilon}$ where $C = 60$ and $\epsilon = 0.001$.

explored for the length and loss volume of a loss period for the discrete process in Section IV.

B. Permissible Correlation Functions

When choosing a correlation function for the analysis, two demands must be satisfied. First, the correlation function should model well the actual video data. Appropriate functions for modeling the correlation function of the “Mobile” clip (available from [14]) are explored in [6]. Second, conditions for the continuous process are given in [11], stating that the process should be a stationary, ergodic Gaussian random process with zero mean and a twice differentiable correlation function such that for $|t| \leq t_0$:

$$|\rho''(0) - \rho''(t)| \leq \psi(|t|), \quad (4)$$

where $\psi(|t|)$ is a non-decreasing and continuous function for $|t| \leq t_0$, $\psi(0) = 0$. This defines the permissible correlation functions. It is found in [11] that the function $\psi(t) = C/|\log |t||^{1+\epsilon}$, $\epsilon > 0$ satisfies the required restriction placed on $\psi(t)$.

The inequality in (4) is plotted in Fig. 3 for the functions e^{-t} and e^{-t^2} to test if these functions are permissible. As can be seen in the figure, the condition is fulfilled for both of these functions, and they are suitable choices for the analysis based on the second requirement.

However, even though this figure shows that the chosen functions are permissible, preliminary calculations showed non-converging integrals for the λ -constants for e^{-t} , as is shown next.

C. Study of Two Permissible Correlation Functions

This section starts with the calculation of the λ -constants with the correlation function $\rho(t) = e^{-t}$. This gives the following expression for the spectral density:

$$f(\lambda) = \frac{2}{\pi} \int_0^\infty \cos(\lambda t) e^{-t} dt = \frac{2}{\pi} \frac{1}{1 + \lambda^2}$$

and hence for the λ_k constants:

$$\lambda_k = \frac{2}{\pi} \int_0^\infty \lambda^k \frac{2}{\pi} \frac{1}{1 + \lambda^2} d\lambda.$$

This integral does not converge when $k = 1, 2$. Hence, the distribution of an excursion can not be found for this correlation function, even though it is a permissible correlation function.

Next, the calculation of the λ -constants using the correlation function $\rho(t) = e^{-t^2}$ is shown. This gives the following expression for the spectral density:

$$f(\lambda) = \frac{2}{\pi} \int_0^\infty \cos(\lambda t) e^{-t^2} dt = \frac{e^{-\frac{1}{4}\lambda^2}}{\sqrt{\pi}}$$

and hence for the λ_k constants:

$$\lambda_k = \frac{2}{\pi} \int_0^\infty \lambda^k \frac{e^{-\frac{1}{4}\lambda^2}}{\sqrt{\pi}} d\lambda.$$

The λ_k -constants will then be equal to: $\lambda_0 = 1$, $\lambda_1 = \frac{2}{\sqrt{\pi}}$ and $\lambda_2 = 2$.

The results based on the limit distributions are unfortunately of limited value due to the restrictions on the correlation functions, and the problems of computing the λ -values even for permissible functions. Appropriate correlation functions computed from the video traces found in [6] can therefore not be employed for estimation of the limit distributions and the permissible function $\rho(t) = e^{-t^2}$ is employed for comparison to the discrete process in Section IV. Because of the shortcomings of the continuous process, a numerical approach to characterizing the loss volume of a loss period for a discrete process is studied in the next section, together with results from simulations.

III. CHARACTERISTICS OF LOSS PERIODS

In this section, the distribution of the length of a loss period for the discrete process as found in [6] is described. Also, the distribution of the loss volume of a loss period is found using both a numerical approach and simulations.

A. Length of Loss Periods

In [6] it was shown that the distribution of the length of a loss period for an aggregated video stream modeled as a multivariate Gaussian process can be estimated using characteristics of a basic stream, also modeled as a multivariate Gaussian process.

The probability of exceeding a threshold b for the aggregated process \mathbf{Y} is then equal to the probability of exceeding the threshold a for the basic process \mathbf{X} , where $a = \frac{b}{\sqrt{n}} - \mu_X(\sqrt{n} - 1)$. Hence:

$$\begin{aligned} & Pr[b \leq Y_1 \leq \infty, b \leq Y_2 \leq \infty, \dots, b \leq Y_m \leq \infty] \\ &= Pr\left[\frac{b}{\sqrt{n}} - \mu_X(\sqrt{n} - 1) \leq X_1 \leq \infty, \dots, \right. \\ &\quad \left. \dots, \frac{b}{\sqrt{n}} - \mu_X(\sqrt{n} - 1) \leq X_m \leq \infty\right] \quad (5) \end{aligned}$$

where n is the number of basic processes in the aggregate and μ_X is the expectation of the basic process.

An expression for the complementary CDF for the number of consecutive losses, $Pr[M_{\mathbf{X},a} > m]$ is found, where $M_{\mathbf{X},a}$

denotes the number of consecutive exceedances for the process \mathbf{X} over the threshold a :

$$\begin{aligned} & Pr[M_{\mathbf{X},a} > m] \\ &= \frac{Pr[X_1 > a, \dots, X_{m+1} > a] - Pr[X_0 > a, \dots, X_{m+1} > a]}{Pr[X_1 > a] - Pr[X_0 > a, X_1 > a]}. \end{aligned}$$

From the complementary CDF, moments of the length of a loss period were computed, using the package *mvtnorm* [15] in R [16] for calculating the probability in (5). In this paper, the correspondence between the moments of the length of a loss period for the discrete process and the length of an excursion for the continuous process is investigated.

B. Loss Volume in a Loss Period

The moments of the loss volume in a loss period, or loss volume in short, can be employed for estimating the packet loss in a bufferless network node. To the best of our knowledge, no exact results exist for the loss volume for a discrete, multivariate normal distribution. In this section, an approximate numerical approach for estimating the loss volume for the discrete process is developed.

The distribution of the loss volume should be conditioned on that the frame immediately before and after a loss period are both below the threshold. It is not straightforward to condition on them being below the threshold, so instead several cases are investigated in the following. The moments of the loss volume are of interest:

$$E[(X_1 - a + \dots + X_m - a)^k | X_0 = x_0, X_1 > a, \dots, X_m > a, X_{m+1} = x_{m+1}]. \quad (6)$$

This expectation can not be found using the *mvtnorm* package in R. However, a function *qsimvnef* in Matlab is available from [17], using the algorithm from [12], for estimating the MVN expectation for an arbitrary expectation function.

The distribution:

$$Pr[X_1 = x_1, \dots, X_m = x_m | X_0 = x_0, X_{m+1} = x_{m+1}] \quad (7)$$

can easily be found using the results from the conditional multivariate distribution [18]. Including the final condition, $X_1 > a, \dots, X_m > a$, is then a matter of normalization.

$$\begin{aligned} & f_{\mathbf{X}}(x_1, \dots, x_m | X_0 = x_0, X_1 > a, \dots, X_m > a, X_{m+1} = x_{m+1}) \\ &= \frac{f_{\mathbf{X}}(x_1, \dots, x_m | X_0 = x_0, X_{m+1} = x_{m+1})}{Pr[X_1 > a, \dots, X_m > a | X_0 = x_0, X_{m+1} = x_{m+1}]}. \end{aligned}$$

The conditional distribution in (7) is rewritten as:

$$f_{\mathbf{C}}(\mathbf{C}_1 | \mathbf{C}_2 = \mathbf{c})$$

where

$$\mathbf{C}_1 = \begin{bmatrix} X_1 \\ \cdot \\ \cdot \\ X_m \end{bmatrix}, \mathbf{C}_2 = \begin{bmatrix} X_0 \\ X_{m+1} \end{bmatrix}$$

and

$$\mathbf{c} = \begin{bmatrix} x_0 \\ x_{m+1} \end{bmatrix}.$$

Results for conditional multivariate normal distributions given e.g., in [18] are then employed in the following.

For our process, the mean vectors have elements:

$$\boldsymbol{\mu}_1 = \begin{bmatrix} \mu_{X_1} \\ \mu_{X_2} \\ \cdot \\ \cdot \\ \mu_{X_m} \end{bmatrix} \quad \text{and} \quad \boldsymbol{\mu}_2 = \begin{bmatrix} \mu_{X_0} \\ \mu_{X_{m+1}} \end{bmatrix}$$

and the covariance matrix has elements:

$$\begin{aligned} \Sigma_{11} &= E[\mathbf{C}_1 \mathbf{C}_1^T] \\ \Sigma_{12} &= [E[\mathbf{C}_1 X_0] \quad E[\mathbf{C}_1 X_{m+1}]] \\ \Sigma_{21} &= \begin{bmatrix} E[X_0 \mathbf{C}_1^T] \\ E[X_{m+1} \mathbf{C}_1^T] \end{bmatrix} \end{aligned}$$

and

$$\Sigma_{22} = \begin{bmatrix} E[X_0 X_0] & E[X_0 X_{m+1}] \\ E[X_0 X_{m+1}] & E[X_{m+1} X_{m+1}] \end{bmatrix}.$$

Then the distribution of \mathbf{C}_1 conditioned on $\mathbf{C}_2 = \mathbf{c}$ is multivariate normal $(\mathbf{C}_1 | \mathbf{C}_2 = \mathbf{c}) \sim N(\boldsymbol{\mu}, \Sigma)$ with mean vector

$$\boldsymbol{\mu} = \boldsymbol{\mu}_1 + \Sigma_{12} \Sigma_{22}^{-1} (\mathbf{c} - \boldsymbol{\mu}_2)$$

and covariance matrix

$$\Sigma = \Sigma_{11} - \Sigma_{12} \Sigma_{22}^{-1} \Sigma_{21}.$$

The expectation function in (6) can now be evaluated numerically. This gives the moments of the sum of exceedances for a given length of the loss period. To find the overall moments, the expectations are unconditioned using the probability density function of the length of a loss period as found in [6].

The k -th moment for the loss volume is then found as:

$$E(S^k) = \sum_{m=1}^{\infty} E \left[\left(\sum_{j=1}^m X_j - a \right)^k | M = m \right] \cdot Pr[M = m]$$

where S is the loss volume of a loss period and M is the length of a loss period.

C. Numerical and Simulation Results

The package *mvtnorm* [15] in R [16] can generate multivariate normal variates with a given mean vector and covariance matrix. The loss period characteristics over a given threshold can then easily be estimated from these variates using simulations. 20 different samples are generated, with 3000 variates in each. The simulation results can be used for validation of the numerical method.

The first moment of the length of a loss period from simulation including Student's t -confidence intervals, is shown in Fig. 4 together with the numerical results from [6], for the covariance function e^{-h^2} . As can be seen in the figure, the results overlap completely for the numerical computation and simulation.

The first moment of the loss volume is shown in Fig. 5, where the results are found from numerical computation and simulation. Three different sets of results are shown, varying

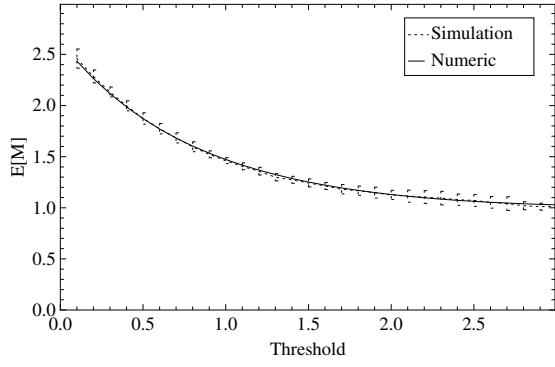


Fig. 4. First moment of the length of a loss period from numerical computation and simulation.

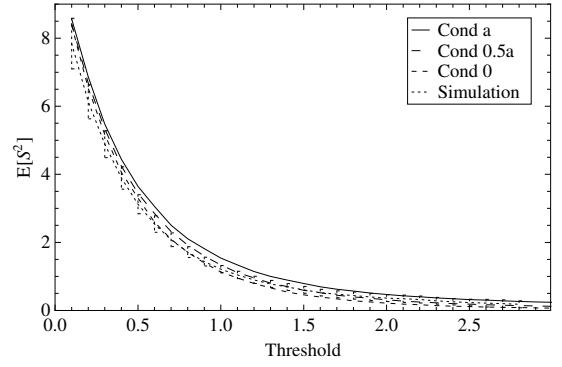


Fig. 6. Second moment of the loss volume in a loss period from numerical computation and simulation.

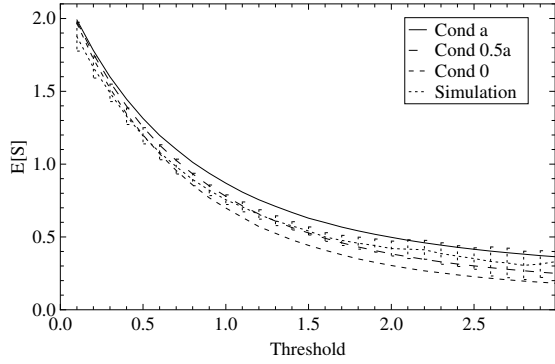


Fig. 5. First moment of the loss volume in a loss period from numerical computation and simulation.

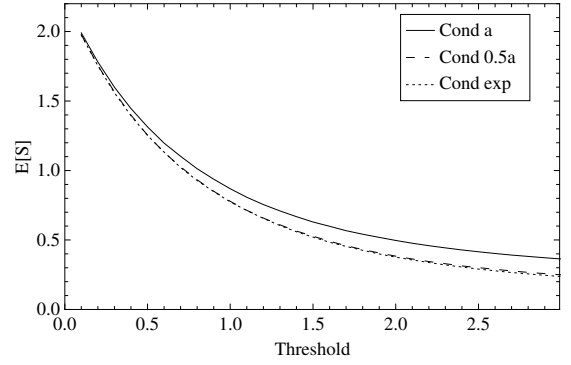


Fig. 7. First moment of the loss volume in a loss period from numerical computation.

the condition on the frames before and after the loss period, with $x_0, x_{m+1} = a$ as the worst case and $x_0, x_{m+1} = 0$ as the best case in terms of a smaller first moment. $x_0, x_{m+1} = 0.5a$ gives the best correspondence to the simulation results. It is clear that decreasing the condition values influences the expectation. Conditioning on $x_0, x_{m+1} = a$ gives too high moments for the loss volume as compared to simulations, while the lowest condition value gives a smaller loss volume than the loss volume from simulations for high thresholds.

The second moment of the loss volume from simulations, including confidence intervals are shown in Fig. 6, together with the results from the numerical computation. Similar discrepancies as for the first moment are observed.

Finally, to overcome the discrepancies due to conditioning on explicit values of X_0 and X_{m+1} , conditioning on the expected values of X_0 and X_{m+1} given that they are below the threshold are employed. Then:

$$x_0 = E[X_0 | X_0 < a, X_1 > a]$$

$$x_{m+1} = E[X_{m+1} | X_m > a, X_{m+1} < a].$$

The results are given in Fig. 7, and show that conditioning on the expected value is very close to conditioning on $x_0, x_{m+1} = 0.5a$, where the latter is a simpler approach.

IV. COMPARISON OF LOSS PERIOD AND EXCURSION

In order to check the agreement between characteristics of the continuous process and the discrete process, the quantiles for loss within a certain percent are investigated. The focus is on 5, 3 and 1 % loss. The quantiles are found for the standard normal distribution $N(0, 1)$ as 1.645 for 5% loss, 1.881 for 3 % loss, and 2.326 for 1% loss.

Acceptable loss is typically below 3%, meaning that thresholds above 1.8 are of highest interest. Whether the correspondence between the moments for the continuous process and the discrete process over these thresholds is satisfactory or not should then be investigated.

The limit distributions, $P_1(v)$, $P_2(v)$ and $P_3(v)$ for the continuous process with correlation function $\rho(t) = e^{-t^2}$ can now be estimated for different thresholds. A comparison between the first moments of the length and volume of an excursion from the continuous model and likewise for the discrete process using numerical evaluation of the multivariate normal integral are shown in Fig. 8, with correlation function $\rho(h) = e^{-h^2}$ for the discrete process.

The results from [11] are valid only when the threshold $r \rightarrow \infty$, which explains the discrepancies for low thresholds in Fig. 8. For thresholds higher than approximately 1.5, the results for the discrete and continuous processes are comparable, covering the interesting range of the thresholds (> 1.8) for

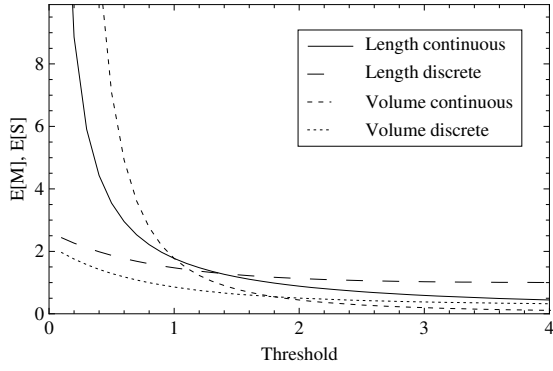


Fig. 8. The first moments of the length and loss volume of a loss period by numerical computation, continuous and discrete process.

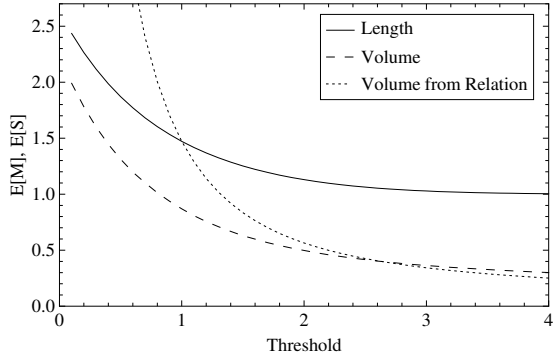


Fig. 9. The first moment of the length and loss volume of a loss period by numerical computation, together with the loss volume from the relation.

which the loss probability is acceptable. Next, the first moment of the length of a loss period for the continuous process tends to zero for high thresholds while for the discrete process, it is conditioned on a loss event and the first moment of the length is always higher than 1.

A. Relation Between Length and Volume

For the continuous Gaussian process, a relation between the length and loss volume of an excursion exists, as shown in (3). In this section, it is investigated if this relation is valid at high thresholds for a discrete process as well.

As a first step, the moments of the length of a loss period are found for the discrete model using the MVNI integral. The first moment of the loss volume is then calculated from the length using (3), and the results are shown in Fig. 9, together with the first moment of the loss volume found from the numerical method, conditioning on $x_0, x_{m+1} = a$.

As can be seen in the figure, the relation between the length and volume of an excursion for the continuous process is a good approximation also in the discrete case. Estimating the loss volume from the relation gives almost identical first moment as for the numerical estimation at high thresholds, using the condition $x_0, x_{m+1} = a$. This means that the first moment of the loss volume estimated from the relation is a bit higher than the loss volume from simulations.

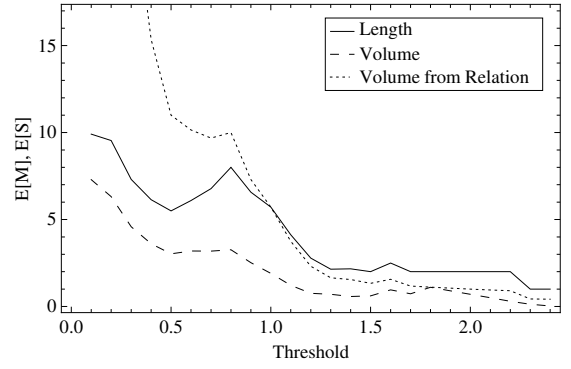


Fig. 10. The first moment of the length of a loss period and the normalized loss volume from the Mobile trace, together with the loss volume found from the relation.

Next, the first moment of the length and loss volume of a loss period from direct inspection of the Mobile trace is shown in Fig. 10, together with the loss volume calculated using the relation between the length and the volume. For high thresholds, the relation gives a close approximation, as was also seen for the discrete process.

V. EXPECTED LENGTH OF LOSS PERIOD AND EXCURSION FROM LITTLE

As an alternative to finding the first moment of the length of a loss period and an excursion, Little's formula [13] can be used to estimate the average length, when the intensity into the loss area is known. Little's formula gives a relation between the average number in a system state, the arrival intensity into the state and the average sojourn time in the state.

For the discrete process, the intensity into the loss area, Λ_D , is known as the probability of having a frame larger than the threshold when the previous frame was below the threshold. This is given as:

$$\begin{aligned} \Lambda_D &= Pr[X_1 > a, X_0 < a] \\ &= Pr[X_1 > a] - Pr[X_0 \geq a, X_1 > a]. \end{aligned}$$

The expected length of a loss period (\bar{W}_D) is then found using the intensity into the loss area (Λ_D) and the expected number in the loss state (\bar{L}_D), where the latter is merely the probability of being in the loss state, given as $Pr[X_0 > a]$.

$$\bar{W}_D = \frac{\bar{L}_D}{\Lambda_D} = \frac{Pr[X_0 > a]}{Pr[X_1 > a] - Pr[X_0 > a, X_1 > a]}.$$

For a continuous process, the intensity into the loss area, Λ_C , is given in [19] and [10]:

$$\Lambda_C = \frac{1}{2\pi} \cdot \sqrt{\frac{-\rho''(0)}{\rho(0)}} \cdot e^{(-\frac{a^2}{2\rho(0)})} = \frac{1}{2\pi} \cdot \sqrt{-\rho''(0)} \cdot e^{(-\frac{a^2}{2})}$$

for the threshold a .

Using Little's formula again then gives:

$$\bar{W}_C = \frac{\bar{L}_C}{\Lambda_C}$$

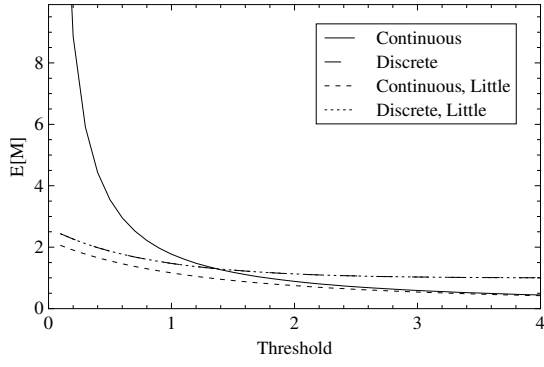


Fig. 11. First moment of the length of a loss period and length of an excursion, together with the results found using Little's formula.

where the probability of being in the loss state is taken from the standard normal distribution for the given threshold a .

The results from using Little's formula on the discrete and continuous processes with correlation function $\rho(h) = e^{-h^2}$ and $\rho(t) = e^{-t^2}$ respectively are shown in Fig. 11 together with the results using the MVNI and the first moment of the excursion length from [11]. As can be seen, the results are identical as for the numerical evaluation for the discrete process. This means that Little's formula gives a very simple approach to finding the expected length of a loss period. For the continuous process, the difference between the moments found from Little and found using the limit distribution from [11] is large for low thresholds, but coincides for thresholds higher than 2.0. This is as expected since the limit distribution is valid only for high thresholds.

VI. THE APPROXIMATE LOSS WITH A SMALL BUFFER

In a bufferless system, the bit loss is estimated by the distribution of the loss volume in a loss period. Next, when the buffer size in a node is finite and relatively small, the loss in a loss period is determined by the buffer size, the buffer content at the end of the loss period, and the loss volume of a loss period in a bufferless system. Loss with a small buffer can then be approximated from the characteristics of the bufferless system.

The excess capacity in a non-loss period is the unused capacity at a time instant. The excess volume (V) is then defined as the accumulated excess capacity in a non-loss period and gives the available capacity that can be used for emptying the buffer before the next loss period. When a non-loss period has a larger excess volume than the remaining buffer content at the end of a loss period, the loss with a small buffer can be found from the loss volume in a loss period in the bufferless system, since the buffer is then always empty at the beginning of a new loss period.

The probability of an empty buffer at the start of a loss period for given thresholds and buffer sizes is therefore investigated. The buffer size is denoted by z and the buffer content is denoted by U . The buffer content at the end of a

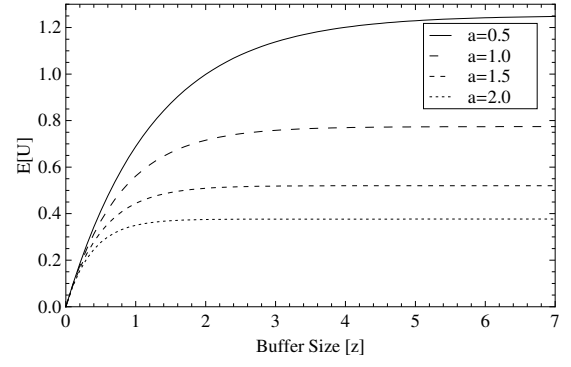


Fig. 12. Expected buffer content at the end of a loss period, for different thresholds a .

loss period is then given as $U = \min(z, S)$, where S is the loss volume of a loss period in the bufferless model.

The expected buffer content at the end of a loss period is then:

$$E[U] = P(S \geq z) \cdot z + P(0 < S < z) \cdot E[S|0 < S < z].$$

The expected buffer content is shown in Fig. 12 for different buffer sizes and thresholds.

The excess volume in a non-loss period can be found numerically using the same procedure as for the loss volume of a loss period. The probability of the excess volume in a non-loss period being larger than the remaining buffer content at the end of a loss period is then given as:

$$\begin{aligned} Pr[V > U] &= \int_{u=0}^z Pr[V > U|U = u] \cdot Pr[U = u] du \\ &= \int_{u=0}^z \int_{v=u}^{\infty} f_U(u) f_V(v) du \end{aligned}$$

where the density function is $f_U(u)$ for the remaining content and $f_V(v)$ for the excess volume, respectively. It is assumed that the remaining buffer content and the excess volume are independent. For the cases studied, the mean and variance of S and V are known. Both of them have a coefficient of variation around 1, and are therefore modeled with an Exponential distribution. The remaining buffer content will have the same distribution as the loss volume for $U < z$, and be equal to z for $U = z$.

The probability of an excess volume in a non-loss period being larger than the remaining buffer content at the end of a loss period for thresholds equal to 0.5-2.0 is shown in Fig. 13. As can be seen, the probability that the buffer is empty at the beginning of a loss period is high for high thresholds.

When it is justified that the probability of an empty buffer at the beginning of a loss period is high, the amount of loss (S_{finite}) is given by $S_{finite} = \max(S - z, 0)$. The expected loss is then given as:

$$E[S_{finite}] = P(S > z) \cdot (E[S|S > z] - z) + P(S \leq z) \cdot 0.$$

The expected loss is shown in Fig. 14(a), for thresholds from 0.5 to 2.0. Clearly, even a very small buffer significantly reduces the expected loss.

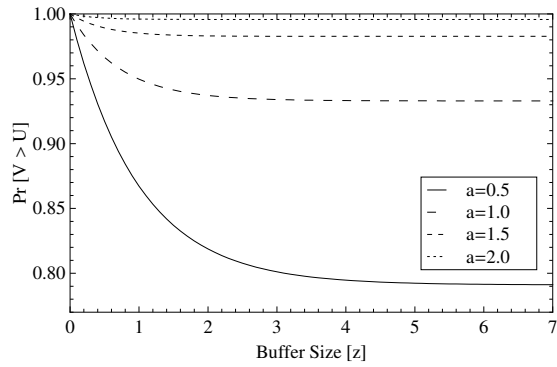
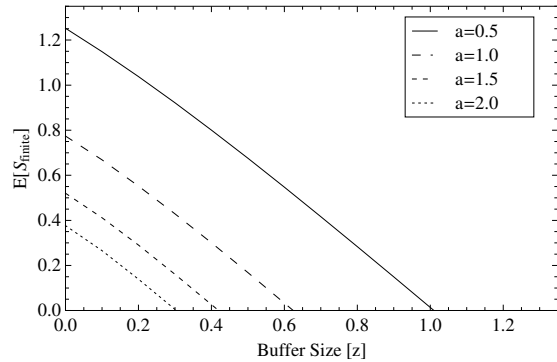
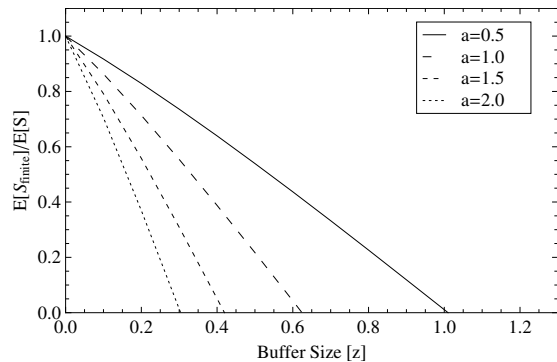


Fig. 13. The probability of the excess volume in a non-loss period being larger than the remaining buffer content at the end of a loss period, for different thresholds a .



(a) Expected loss as function of buffer size



(b) The reduction in loss by introduction of a buffer.

Fig. 14. Expected loss with a small buffer, and the corresponding reduction in loss compared to the bufferless case.

Finally, the reduction in the expected loss in a loss period by introduction of a small buffer is given in Fig. 14(b) as $E[S_{finite}]/E[S]$. This can be interpreted as the gain in terms of reduced loss by including a buffer of the given size.

VII. CONCLUSION

The distribution of the loss volume of a loss period is important for assessing the QoS perceived by the users when a video stream is transmitted through a network. In this paper, a numerical approach to the estimation of the moments of the loss volume is given, when the video traffic is modeled as a discrete multivariate Gaussian process. The distribution

of the loss volume can also be employed for estimating the expected loss in a node with a small buffer, in addition to giving the loss directly in a bufferless node. Comparison of the first and second moments of the length and volume of the excursion/loss period for the continuous and discrete process gives satisfactory correspondence for high thresholds. This is as expected, since the results for the continuous process are only valid for high thresholds. The latter approach is restrictive to which covariance function can be used, and it is therefore not so useful. However, the relation between the length and volume of the excursions for the continuous process is found to hold also for the discrete process for the examples studied.

The numerical computation time for the moments of the loss volume in a loss period is in the order of minutes for each threshold, using a regular PC.

Future work includes estimation of loss in a single stream based on the distribution of loss in the aggregated stream.

REFERENCES

- [1] A. Raake, M. N. Garcia, S. Möller, J. Berger, F. Kling, P. List, J. Johann, and C. Heidemann, "T-V-Model: Parameter-based Prediction of IPTV Quality," in *Proceedings of the IEEE ICASSP '08*, March-April 2008.
- [2] S. Winkler and P. Mohandas, "The Evolution of Video Quality Measurement: From PSNR to Hybrid Metrics," *IEEE Transaction on Broadcasting*, vol. 54, no. 3, pp. 660–668, September 2008.
- [3] S. Mohamed and G. Rubino, "A Study of Real-Time Packet Video Quality Using Random Neural Networks," *IEEE Transactions on Circuits and Systems for Video Technology*, vol. 12, no. 12, pp. 1071–1083, December 2002.
- [4] Y. J. Liang, J. G. Apostolopoulos, and B. Girod, "Analysis of Packet Loss for Compressed Video: Does Burst-Length Matter?" in *Proceedings of the IEEE ICASSP '03*, vol. 5, April 2003.
- [5] I. Norros, "A Storage Model with Self-Similar Input," *Queueing Systems*, vol. 16, no. 3-4, pp. 387–396, September 1994.
- [6] A. Undheim and P. J. Emstad, "Distribution of Loss Periods for Aggregated Video Traffic," in *Proceedings of the ITC Specialist Seminar (ITCSS'18)*, May 2008.
- [7] M. Fidler, Y. Lin, P. J. Emstad, and A. Perkis, "Efficient Smoothing of Robust VBR Video Traffic by Explicit Slice-Based Mode Type Selection," in *Proceedings of the 4th IEEE Consumer Communications and Networking Conference (CCNC)*, January 2007.
- [8] I. F. Blake and W. C. Lindsey, "Level-Crossing Problems for Random Processes," *IEEE Transactions on Information Theory*, vol. 19, no. 3, pp. 295–315, May 1973.
- [9] T. Mimaki and T. Munakata, "Experimental Results on the Level-Crossing Intervals of Gaussian Processes," *IEEE Transactions on Information Theory*, vol. 24, no. 4, pp. 515–519, July 1978.
- [10] D. R. Morgan, "On Level-Crossing Excursions of Gaussian Low-Pass Random Processes," *IEEE Transactions on Signal Processing*, vol. 55, no. 7, pp. 3623–3632, July 2007.
- [11] Y. K. Belyaev and V. P. Nosko, "Characteristics of Excursions Above a High Level for a Gaussian Process and Its Envelope," *Theory of Probability and Its Applications*, vol. 14, no. 2, pp. 296–309, January 1969.
- [12] A. Genz, "Numerical Computation of Multivariate Normal Probabilities," *Journal of Computational and Graphical Statistics*, vol. 1, no. 2, pp. 141–149, June 1992.
- [13] V. B. Iversen, *Data- og teletrafikteori*. Den Private Ingeniørfond, 1999.
- [14] [Online]. Available: <ftp://ftp.tnt.uni-hannover.de/pub/svc/testsequences/>
- [15] A. Genz and F. Bretz, *The mvtnorm Package*, July 2007. [Online]. Available: <http://cran.r-project.org/doc/packages/mvtnorm.pdf>
- [16] R Development Core Team, "R project." [Online]. Available: www.r-project.org
- [17] [Online]. Available: <http://www.math.wsu.edu/faculty/genz/homepage>
- [18] S. F. Arnold, *The Theory of Linear Models and Multivariate Analysis*. Wiley, 1981.
- [19] C. E. Rasmussen and C. K. I. Williamson, *Gaussian Processes for Machine Learning*. MIT Press, 2006.